Comparison of ^{18}F-Fluoro-L-DOPA, ^{18}F-Fluoro-Deoxyglucose, and ^{18}F-Fluorodopamine PET and ^{123}I-MIBG Scintigraphy in the Localization of Pheochromocytoma and Paraganglioma

Henri J. L. M. Timmers, Clara C. Chen, Jorge A. Carrasquillo, Millie Whatley, Alexander Ling, Bastiaan Havekes, Graeme Eisenhofer, Lucia Martiniova, Karen T. Adams, and Karel Pacak*

Context: Besides ^{123}I-metaiodobenzylguanidine (MIBG), positron emission tomography (PET) agents are available for the localization of paraganglioma (PGL), including ^{18}F-3,4-dihydroxyphenylalanine (DOPA), ^{18}F-fluoro-2-deoxy-D-glucose (^{18}F-FDG), and ^{18}F-fluorodopamine (^{18}F-FDA).

Objective: The objective of the study was to establish the optimal approach to the functional imaging of PGL and examine the link between genotype-specific tumor biology and imaging.

Design: This was a prospective observational study.

Intervention: There were no interventions.

Patients: Fifty-two patients (28 males, 24 females, aged 46.8 $\pm$ 14.2 yr): 20 with nonmetastatic PGL (11 adrenal), 28 with metastatic PGL (13 adrenal), and four in whom PGL was ruled out; 22 PGLs were of the succinate dehydrogenase subunit B (SDHB) genotype.

Main Outcome Measures: Sensitivity of ^{18}F-DOPA, ^{18}F-FDG, and ^{18}F-FDA PET, ^{123}I-MIBG scintigraphy, computed tomography (CT), and magnetic resonance imaging (MRI) for the localization of PGL were measured.

Results: Sensitivities for localizing nonmetastatic PGL were 100% for CT and/or MRI, 81% for ^{18}F-DOPA PET, 88% for ^{18}F-FDG PET/CT, 78% for ^{18}F-FDA PET/CT, and 78% for ^{123}I-MIBG scintigraphy. For metastatic PGL, sensitivity in reference to CT/MRI was 45% for ^{18}F-DOPA PET, 74% for ^{18}F-FDG PET/CT, 76% for ^{18}F-FDA PET/CT, and 57% for ^{123}I-MIBG scintigraphy. In patients with SDHB metastatic PGL, ^{18}F-FDA and ^{18}F-FDG have a higher sensitivity (82 and 83%) than ^{123}I-MIBG (57%) and ^{18}F-DOPA (20%).

Conclusions: ^{18}F-FDA PET/CT is the preferred technique for the localization of the primary PGL and to rule out metastases. Second best, equal alternatives are ^{18}F-DOPA PET and ^{123}I-MIBG scintigraphy. For patients with known metastatic PGL, we recommend ^{18}F-FDA PET in patients with an unknown genotype, ^{18}F-FDG or ^{18}F-FDA PET in *SDHB* mutation carriers, and ^{18}F-DOPA or ^{18}F-FDA PET in non-*SDHB* patients. **(*J Clin Endocrinol Metab* 94: 4757–4767, 2009)**

Paragangliomas (PGLs) derive from sympathetic chromaffin tissue in adrenal and extraadrenal abdominal or thoracic locations or from parasympathetic tissue of the head and neck (1). The terms pheochromocytoma and glomus tumor refer to respective adrenal PGL and head and neck PGL (2, 3). The majority of abdominal and thoracic PGLs produce catecholamines (4), whereas head and neck PGLs usually do not. This study focused on sympathetic PGL.

ISSN Print 0021-972X ISSN Online 1945-7197
Printed in U.S.A.

doi: 10.1210/jc.2009-1248 Received June 12, 2009. Accepted September 21, 2009.
First Published Online October 28, 2009
*Author affiliations are shown at the bottom of the next page.

Abbreviations: CT, Computed tomography; DOPA, L-3,4-dihydroxyphenylalanine; FDA, fluorodopamine; FDG, fluoro-2-deoxy-D-glucose; MIBG, metaiodobenzylguanidine; MRI, magnetic resonance imaging; PET, positron emission tomography; PGL, paraganglioma; SDHB, succinate dehydrogenase subunit B; SDHD, succinate dehydrogenase subunit D; suv, standardized uptake value; VHL, von Hippel Lindau.

Accurate tumor localization is critical for guiding the optimal therapeutic approach for PGL, in particular for identification of multiple primary tumors or metastases. Lesions detected by anatomical imaging can be specifically identified as PGL by functional imaging agents that target the catecholamine synthesis, storage, and secretion pathways of chromaffin tumor cells (5). These techniques include [$^{123/131}$I]metaiodobenzylguanidine (MIBG) scintigraphy, 6-[^{18}F]fluoro-L-3,4-dihydroxyphenylalanine (DOPA) positron emission tomography (PET), and 6-[^{18}F]fluorodopamine (FDA) PET. 2-[^{18}F]fluoro-2-deoxy-D-glucose (FDG) PET provides another modality for localization of metastatic PGL, albeit with less tissue specificity than the other functional approaches that target the catecholamine biosynthetic and storage pathways (6–8).

Previous studies on the performance of different functional imaging modalities in PGL yielded discrepant results (8–15). Meaningful comparisons among these studies is hampered by heterogeneous patient sample groups with respect to PGL location (adrenal and extraadrenal abdominal *vs.* thoracic *vs.* head and neck), benign *vs.* malignant PGL, and hereditary *vs.* sporadic PGL. At least 25–30% of patients with PGL have underlying mutations in one of the four known PGL susceptibility genes (16). The various PGL genotypes are increasingly recognized as important determinants of functional imaging results. For example, ^{18}F-FDA PET is superior to ^{123}I-MIBG scintigraphy in the context of von Hippel Lindau (VHL) syndrome (17), whereas ^{18}F-FDG PET is extremely sensitive in metastatic PGL associated with mutations in *succinate dehydrogenase subunit B (SDHB)* (8).

Individually, the PET tracers ^{18}F-FDA, ^{18}F-DOPA, and ^{18}F-FDG have been claimed to be superior to ^{123}I-MIBG for the localization of PGL in the particular clinical contexts of different studies. So far, however, a comprehensive comparison between these tracers within the same patient population has not been performed. In the present study, such a head-to-head comparison was accomplished in a large, heterogeneous group of patients with benign and malignant PGLs of various locations and genotypes. The aim of this study was to establish the optimal approach to the functional imaging of sympathetic PGL and further explore possible links between tumor genotypes and imaging.

Patients and Methods

Patients

Between June 2006 and June 2008, we prospectively studied 53 patients (29 males, 24 females, mean ± SD, aged 46.8 ± 14.2 yr), who were consecutively evaluated for known or suspected PGL. At the time of the study, 20 patients had histologically proven, nonmetastatic PGL (no. p1-20), including 11 with adrenal PGL, seven with extraadrenal abdominal or thoracic PGL, one with bilateral adrenal and an extraadrenal PGL, and one with a catecholamine secreting head PGL. Twenty-eight patients had metastatic PGL (no. m1-28), including 13 with primary adrenal tumors and 15 with primary extraadrenal abdominal or thoracic tumors. Metastatic PGL was defined by the presence of metastatic lesions at sites in which chromaffin tissue is normally absent (18). In four patients, PGL was ruled out by normal biochemical findings (no. n1-4). One patient was excluded from the analysis because a histological diagnosis was still pending. Clinical details of individual patients, including previous treatments, are listed in Tables 1–3.

Twenty-two patients had an underlying mutation of the *SDHB* gene, four of the *succinate dehydrogenase subunit D* (*SDHD*) gene, three of the *rearranged during transfection* protooncogene, and two of the *VHL* gene. Six patients had sporadic tumors, two were not tested, and in 14 patients lacking syndromic features, at least *SDHx* mutations were ruled out. The results of ^{18}F-DOPA PET scanning in the first 11 patients were reported in a previous paper on the usefulness of the administration of carbidopa before scanning (19).

This protocol was approved by the Institutional Review Board of the National Institute of Child Health and Development at the National Institutes of Health. All patients provided written informed consent.

Computed tomography (CT) and magnetic resonance imaging (MRI)

In all 53 patients, CT scans of the neck, chest, abdomen, and pelvis were performed, using LightSpeed Ultra, LightSpeed QX/i (General Electric Healthcare Technologies, Waukesha, WI), and Mx8000 IDT (Philips Medical Systems, Andover, MA) scanners. Section thickness was 2–2.5 mm in the neck and 5 mm through the chest, abdomen, and pelvis. Studies were performed with a rapid infusion of nonionic water-soluble contrast agent as well as oral contrast material.

In 45 patients, additional MRI scans of the neck, chest, abdomen, and/or pelvis were obtained, using 1.5 or 3 Tesla scanners (General Electric Healthcare Technologies and Philips Medical Systems). Phased-array coils were used for neck imaging and either phased array torso or quadrature body coils elsewhere. T1-weighted gradient-echo, and short-τ inversion recovery and/or fat-suppressed fast spin-echo T2-weighted imaging parameters were adjusted to minimize examination time but achieving desired anatomic coverage. Image thickness was 5 mm for neck studies and 5–8 mm for other body regions. Preinjection images were obtained in the axial plane. Studies included injec-

Reproductive and Adult Endocrinology Program (H.J.L.M.T., B.H., L.M., K.T.A., K.P.), Eunice Kennedy Shriver National Institutes of Child Health and Human Development, and Departments of Nuclear Medicine (C.C.C., J.A.C., M.W.) and Diagnostic Radiology (A.L.), Warren G. Magnuson Clinical Center, National Institutes of Health, Bethesda, Maryland 20892; Department of Endocrinology (H.J.L.M.T.), Radboud University Nijmegen Medical Centre, 6500 HB Nijmegen, The Netherlands; Nuclear Medicine Section (J.A.C.), Department of Radiology, Memorial Sloan Kettering Cancer Center, New York, New York 10021; Department of Internal Medicine (B.H.), Division of Endocrinology, University Hospital Maastricht, 6202 AZ Maastricht, The Netherlands; and Institute of Clinical Chemistry and Laboratory Medicine and the Department of Medicine (G.E.), University of Dresden, 01307 Dresden, Germany

TABLE 1. Nonmetastatic PGL

Patient no.	Sex	Reason for evaluation	Age at diagnosis (yr)	Location primary tumor	Hypersecretion	Genotype	Time until metastases (yr)	Locations of metastases	Previous treatment	Imaging results: true positive lesions, n				
										CT/MRI	^{18}F-DOPA	^{18}F-FDA	^{123}I-MIBG	^{18}F-FDG
p01	F	Monitor primary	51	R paraaortic abdomen	NE	*SDHB*	na	na	MIBG	1	0	1	1	1
p02	F	Suspected primary	53	R adrenal	NE	Negative for *SDHx/RET*	na	na		1	1	1	1	1
p03	F	Suspected recurrence	33	R+L adrenal	E	*RET*	na	na	Res primary	1	1	0	1	0
p04	F	Suspected primary	56	R adrenal	NE+E	Negative for *SDHx/RET*	na	na		1	1	0	1	1
p05	M	Suspected primary	31	L paraaortic abdomen	DA	*SDHB*	na	na		1	0	1	1	1
p06	M	Suspected primary	58	L adrenal	NE+E	Negative for *SDHx*	na	na		1	1	1	1	1
p07	M	Suspected primary	59	R paraaortic abdomen	NE	Negative for *SDHB*	na	na		1	1	1	1	1
p08	F	Suspected recurrence	18	Mult extraadrenal abdomen	NE	Sporadic	na	na		2	1	0	0	1
p09	F	Suspected recurrence	16	R jugular ganglion	NE	Sporadic	na	na	Res+RT primary	1	1	1	1	1
p10	F	Suspected primary	52	L adrenal	NE+E	Negative for *SDHx*	na	na		1	1	1	1	1
p11	M	Suspected primary	72	R adrenal	NE+E	Negative for *SDHx*	na	na		1	1	1	1	1
p12	M	Monitor primary		R+L adrenal, mediastinal	NE+DA	*SDHD*	na	na		2	1	2	1[a]	2
p13	M	Monitor primary	49	Mediastinal	NE+DA	*SDHD*	na	na	Partial res primary	1	1	1	1	1[a]
p14	M	Suspected primary	22	R+L adrenal, R carotid	NE	*VHL*	na	na		3	3	3	3	3
p15	M	Rule out primary	61	L extraadrenal abdomen	DA	*SDHB*	na	na		1	0	0	0	1
p16	M	Rule out primary	34	Mult extraadrenal abdomen	NE	*SDHB*	na	na		3	3	3[a]	2[a]	2[a]
p17	F	Suspected primary	44	R adrenal	NE+E	Negative for *SDHx*	na	na		1	1	0	0	1
p18	F	Suspected primary	48	R adrenal	NE+E	Negative for *SDHx/RET*	na	na		1	1	1	1	1
p19	M	Suspected primary	36	L adrenal	NE+E	Negative for *SDHx*	na	na		1	1	1	1	1
p20	F	Suspected primary	39	R adrenal	NE+E	*RET*	na	na		1	1	1	1	1

DA, Dopamine; E, epinephrine; F, female; M, male; MIBG, ^{131}I-MIBG treatment; mult, multiple; na, not available, NE, norepinephrine; R, right; res, surgical resection; RET, rearranged during transfection; RT, radiotherapy; susp, suspicion.

[a] Additional false-positive lesion(s).

TABLE 2. Metastatic PGL

Patient no.	Sex	Reason for Evaluation	Age at diagnosis (yr)	Location primary tumor	Hypersecretion	Genotype	Time until metastases (yr)	Locations metastases	Previous treatment	Imaging results: lesions detected, n				
										CT/MRI	^{18}F-DOPA	^{18}F-FDA	^{123}I-MIBG	^{18}F-FDG
m01	M	Monitor metastases	27	L extraadrenal abd		*SDHB*	0	Abd, me, b	Res primary; CT	7	3	7	5	5
m02	F	Monitor metastases	23	Paraaortic abd	NE	*SDHB*	0,3	Abd, b	Res primary; CT	4	8	4	3	6
m03	M	Monitor metastases	22	R adrenal	NE	*SDHD*	10,3	Abd, li, me, b	Res primary; MIBG	9	2	3	3	8
m04	M	Monitor metastases	10	R paraadrenal	NE+DA	*SDHB*	8,4	Abd, lu, li, b, n	MIBG	16	1	23	13	21
m05	M	Susp metastases	39	R adrenal	NE+DA	Neg for *SDHx*	14,7	Abd, me, b	Res primary	16	21	19	16	13
m06	F	Monitor metastases	33	R+L adrenal	NE+E	*RET*	6,2	Abd, li, b	Res primary; MIBG	12	18	18	11	1
m07	M	Susp metastases	40	L paraaortic abd	NE	*SDHB*	3,9	li	Res primary	7	0	0	2	4
m08	M	Monitor metastases	40	R adrenal	NE+DA	Neg for *SDHx*	5,4	lu, b	Res primary; CT; MIBG	4	2	1	2	2
m09	F	Susp metastases	46	Retropancreatic	NE+DA	*SDHB*	0	b	Res primary	7	16	9	1	9
m10	F	Monitor metastases	20	Zuckerkandl	NE+DA	Sporadic	0	Abd, li, b	Debulking primary; CT; RT sacrum	5	11	0	2	9
m11	F	Monitor metastases	39	R adrenal	NE+E	Sporadic	7	Abd, lu, me, li	Res primary; CT; MIBG	7	16	12	5	8
m12	M	Monitor metastases	52	L adrenal	NE+E	*VHL*	20	Abd, li	Res primary; CT; MIBG	1	7	7	1	0
m13	M	Monitor metastases	42	L pararenal		*SDHB*	0	Lu, b	Res primary+lung met; CT; MIBG	3	0	0	0	4
m14	F	Monitor recurrence	22	Me+extraadrenal abd	NE	*SDHB*	5	b	Re-res primary	0	3	2	0	0
m15	M	Monitor metastases	32	L paraaortic abd	NE+DA	*SDHB*	4	Abd, me	Res primary	9	0	0	0	14
m16	M	Monitor metastases	41	R adrenal	E	Sporadic	15	b	Re-res primary	0	5	4	2	2
m17	F	Monitor metastases	37	L paraaortic abd	NE	Sporadic	9	Abd	Res primary, res recurrence, res mets	0	3	1	1	0
m18	F	Monitor metastases	18	L adrenal+L carotid	NE	*SDHB*	13	b, me	Res primary	20	7	30	26	31
m19	F	Monitor metastases	51	L adrenal	NE	Neg for *SDHx*	1	Lu, b	CT	4	2	1		4
m20	M	Monitor metastases	25	Mediastinum		*SDHB*	2	Lu, b	Res+RT primary, res lung meta	11	0	16	1	16
m21	M	Monitor metastases	11	R pararenal	NE	*SDHB*	8	b	Res primary	2	0	2	2	2
m22	M	Susp recurrence	36	R adrenal	NE	Neg for *SDHx*	10	a/p	Res primary	4	5	6	3	3
m23	F	Monitor metastases	37	Pelvic	NE+DA	*SDHB*	0,8	a/p, li	CT, meta res	0	0	0		
m24	F	Monitor metastases	51	L adrenal	NE	Neg for *SDHx*	5	Lu, b, a/p, li	res primary	14	21	22	7	10
m25	M	Monitor metastases	14	R adrenal		*SDHB*	2	b, li, a/p	Res+RT primary, CT	19	10	22	14	16
m26	F	Susp metastases	48	Mediastinum or L/R carotid		*SDHD*	?	Lu, li, me, neck	Res carotid body tumors	9	13	5	2	8
m27	M	Monitor metastases	24	L adrenal	NE	*SDHB*	0	b, a/p	CT, MIBG	20	0	29		12
m28	M	Monitor metastases	30	R extraadrenal abd		*SDHB*	17	b	res primary, meta res	1	0	0	0	1

abd, Abdominal lymph node; b, bone; DA, dopamine; E, epinephrine; F, female; li, liver; lu, lung; M, male; me, medistinum; meta, metastases; MIBG, ^{131}I-MIBG treatment; n, neck; NE, norepinephrine; R, right; res, surgical resection; RET, rearranged during transfection; RT, radiotherapy; susp, suspicion.

TABLE 3. PGL ruled out or diagnosis pending

Patient no.	Sex	Reason for evaluation	Age at diagnosis (yr)	Location primary tumor	Hypersecretion	Genotype	Time until metastases (yr)	Locations metastases	Previous treatment	Imaging results: false-positive lesions, n				
										CT/MRI	^{18}F-DOPA	^{18}F-FDA	^{123}I-MIBG	^{18}F-FDG
PGL ruled out														
n01	F	Rule out primary				Not tested				1				1
n02	F	Susp recurrence	38	R carotid		*SDHB*			Res primary					
n03	M	Rule out primary				*SDHB*				1	1			1
n04	M	Rule out recurrence	76	L adrenal	NE	Not tested								

F, Female; M, male; NE, norepinephrine; R, right; res, resection; susp, suspicion.

tion of a gadolinium-^{111}In-diethylenetriamine-pentacetic acid contrast agent, using fat-suppressed T1-weighted gradient-echo imaging, generally in both axial and coronal planes.

Functional imaging

^{123}I-MIBG scintigraphy, ^{18}F-FDG PET/CT, ^{18}F-DOPA PET, and ^{18}F-FDA PET/CT were performed as described previously (8, 19). ^{18}F-DOPA PET scanning was preceded by oral administration of 200 mg carbidopa, a peripheral aromatic amino acid decarboxylase inhibitor (19). All patients underwent ^{18}F-DOPA PET and ^{18}F-FDA PET/CT, all but one underwent ^{18}F-FDG PET/CT, and all but three underwent ^{123}I-MIBG scintigraphy.

Analysis of data

CT and MRI scans were read by a single radiologist who was blinded to results of other imaging studies. Lesions detected by CT and/or MRI that were typical or highly suspicious for PGL were considered positive.

^{18}F-DOPA PET and ^{18}F-FDA PET were each read in blinded fashion by two nuclear medicine physicians during separate reading sessions. Focal areas of abnormal uptake not corresponding to normal physiological sites of accumulation for each of the tracer were considered as lesions. Lesions were graded on a scale of 1–5 (1, not PGL; 2, doubtful; 3, equivocal; 4, probable; 5, definite PGL). Lesions with scores of 4 and 5 were counted as positive findings. Discrepancies were resolved by consensus review.

Lesions detected by CT, MRI, and functional imaging studies were counted in the following three separate body regions: neck, thorax, and abdomen/pelvis. Counts included both soft tissue and bone lesions. If the number of lesions in a region exceeded 10, the count was truncated at 10 to avoid bias toward that patient. Lesions of the head and extremities were not included in the analysis because these areas were not systematically scanned. For this reason, primary nonsecreting head and neck paragangliomas were excluded from the analysis.

Imaging results in individual patients were compared between scans performed within a 3-month interval, with the exception of one patient (no. m4), in whom ^{18}F-FDG PET was performed with a delay of 7 months. In this interval, he did not undergo treatment, and repeat CT showed no additional lesions.

Sensitivities for tumor detection were calculated in reference to two different gold standards. In patients with nonmetastatic PGL, sensitivities were calculated in reference to histopathologically confirmed PGLs. If surgical resection of the culprit lesion(s) resulted in normalization of plasma-free metanephrines without signs of recurrence during follow-up, additional lesions of the chest and abdomen on preoperative imaging were presumed to be false positive. In patients with metastatic PGL, comprehensive histopathological confirmation of all lesions to serve as gold standard for imaging results was not feasible. Instead, the sensitivity for metastases was calculated in reference to lesions detected by CT and/or MRI. The sensitivity for metastases was based on per-region counts as stated above, not on a per-lesion basis.

Sensitivities were analyzed separately in patients with nonmetastatic and metastatic disease. Prompted by earlier findings in patients with *SDHB*-related PGL (8), sensitivities for the detection of metastases were compared between patients with and without underlying *SDHB* mutations.

TABLE 4. Sensitivity

	CT and/or MRI	^{18}F-DOPA	^{18}F-FDA	^{123}I-MIBG	^{18}F-FDG
Nonmetastatic PGL (20 patients)					
In reference to histologically confirmed lesions	100% (26/26)	81% (21/26)	77% (20/26)	77% (20/26)	88% (23/26)
Sensitivities are not significantly different between functional imaging modalities					
	CT and/or MRI	**^{18}F-DOPA^{A}**	**^{18}F-FDA^{B}**	**^{123}I-MIBG^{C}**	**^{18}F-FDG^{D}**
Metastatic PGL (28 patients)					
In reference to lesions on CT and/or MRI		45% (96/211)	76% (161/211)	57% (106/187)	74% (157/211)

A *vs.* B, A *vs.* C, A *vs.* D, B *vs.* C, C *vs.* D: $P < 0.01$; B *vs.* D: $P = 0.760$.

Statistics

Results are given as mean ± SD unless stated otherwise. The McNemar test was used to compare sensitivities between different functional imaging modalities. A χ^2 test was used to compare sensitivities between patients with and without *SDHB* mutations. A two-sided $P < 0.05$ was considered significant. Statistical analysis was performed using Statistical Package for the Social Sciences (SPSS for Windows 12; SPSS Inc., Chicago, IL).

Results

Nonmetastatic PGL

In 20 patients, 26 nonmetastatic PGLs were histopathologically identified. Besides anatomic imaging, all types of functional imaging were performed in all patients. One patient (no. p1) had inadvertently taken 40 mg instead of 200 mg carbidopa before ^{18}F-DOPA PET. Discrepant readings were solved by consensus for two lesions on ^{18}F-DOPA PET.

Of 26 PGLs, all lesions were detected by CT and/or MRI (sensitivity 100%), 21 by ^{18}F-DOPA PET (sensitivity 81%), 20 by ^{18}F-FDA PET/CT (sensitivity 78%), 20 by ^{123}I-MIBG scintigraphy (sensitivity 78%), and 23 by ^{18}F-FDG PET/CT (sensitivity 88%, P = ns, Table 4). Six false-positive lesions were detected. ^{123}I-MIBG scintigraphy showed two false-positive chest lesions in one patient (no. p12). ^{18}F-FDG PET/CT showed three false-positive lesions. In one patient (no. p13), a right inguinal lesion on ^{18}F-FDG PET/CT [maximum standardized uptake value (suv) 4.5] correlated with a 1.9 cm normal-appearing lymph node on CT. In another patient (no. 16), the ^{18}F-FDG PET/CT showed two small foci in the vertebral bodies of T9 (maximum suv 2.6) and L5 (maximum suv 4.2), not correlating with abnormalities on anatomical imaging. Clinical follow-up of 1.5 yr showed no (biochemical) evidence of recurrent or metastatic disease in either of these patients. ^{18}F-FDA PET/CT showed one false-positive lesion (no. 16). There were no false-positive lesions on CT, MRI, and ^{18}F-DOPA PET.

Metastatic PGL

All 28 patients with metastatic PGL underwent anatomical imaging and all types of functional imaging, except for three patients who did not undergo ^{123}I-MIBG scintigraphy, and one patient who did not undergo ^{18}F-FDG PET. In reference to CT and/or MRI region-based sensitivities were: ^{18}F-FDA PET/CT, 76% (161 of 211); ^{18}F-FDG PET/CT, 74% (157 of 211); ^{123}I-MIBG scintigraphy, 57% (106 of 187); and ^{18}F-DOPA PET, 45% (96 of 211). These results were significantly different between the imaging techniques ($P < 0.01$), except between ^{18}F-FDA and ^{18}F-FDG (P = ns, Table 4 and Fig. 1).

In one patient (no. m23), no lesions were detected by any imaging study, who previously underwent metastasectomy. In the remaining patients, one or more lesions were detected by CT and/or MRI in 24 of 27 patients (89%), ^{18}F-FDG PET/CT in 24 of 27 patients (89%), ^{18}F-FDA PET/CT in 22 of 27 patients (81%), ^{18}F-DOPA PET in 20 of 27 patients (74%), and ^{123}I-MIBG scintigraphy in 21 of 25 patients (84%).

In the 28 patients, a total score of 334 lesions was obtained from all anatomic and functional imaging studies by regional analysis. The total score for ^{18}F-FDA PET/CT alone was 246, 211 for CT and/or MRI, 174 for ^{18}F-DOPA PET, and 209 for ^{18}F-FDG PET/CT. Lesion counts were truncated at 10 in 16 regions for ^{18}F-FDA PET/CT, 10 regions for CT and/or MRI, 10 regions for ^{18}F-FDG PET/CT, and nine regions for ^{18}F-DOPA PET. In the 25 patients who underwent ^{123}I-MIBG scintigraphy, 122 lesions were counted and were truncated in three regions.

Functional imaging sensitivities for metastatic lesions were compared between 15 patients with and 13 patients without mutations of the *SDHB* gene. In *SDHB* patients, ^{18}F-FDG PET/CT detected metastases in all patients, whereas several other scans were false negative: in three patients (no. m13, m15, m28), no lesions were visualized by ^{18}F-FDA, ^{18}F-DOPA, or ^{123}I-MIBG, in another (no. m7), no lesions were detected by ^{18}F-FDA and ^{18}F-DOPA,

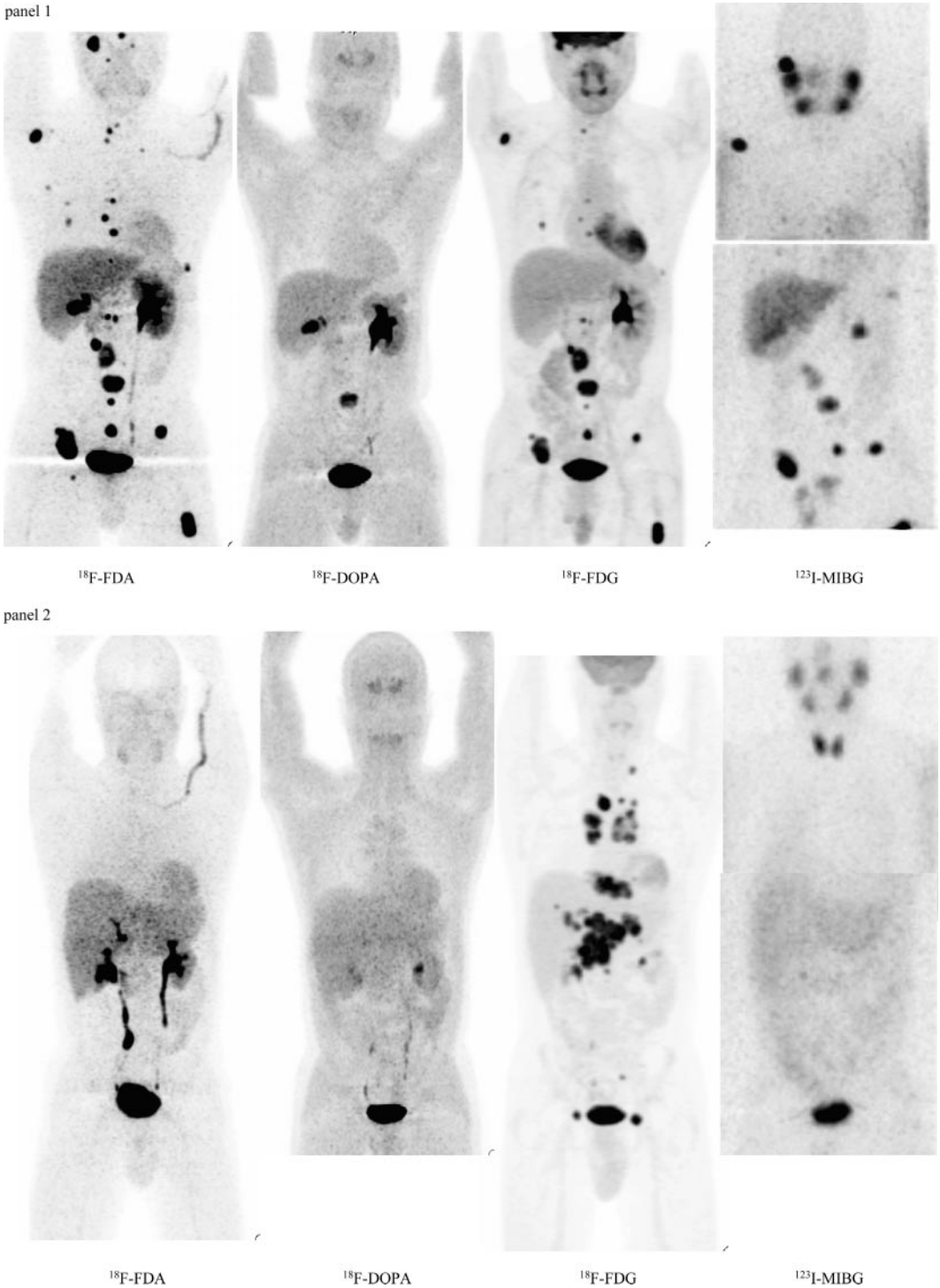

FIG. 1. Functional imaging in patients no. m4 with metastatic *SDHB* PGL (panel 1), m15 with metastatic *SDHB* PGL (panel 2), and m6 with metastatic *RET* PGL (panel 3). Anteriorly reprojected images.

and in three (no. m20, 21, and m27) ^{18}F-DOPA was false negative (^{123}I-MIBG not done in no. m27). In non-*SDHB* patients, a false-negative ^{18}F-FDG scan was obtained in one patient (no. m12 with *VHL* mutation), and ^{18}F-FDA was negative in one patient (no. m10, sporadic). Using CT/MRI as a gold standard, lesion-based sensitivities in *SDHB vs.* non-*SDHB* patients are given in Table 5. In *SDHB* patients, ^{18}F-FDA and ^{18}F-FDG have a higher sensitivity (82 and 83%) than ^{123}I-MIBG (57%) and ^{18}F-DOPA (20%). In non-*SDHB* patients, ^{18}F-DOPA has the best sensitivity (93%), followed by ^{18}F-FDA (76%), ^{123}I-MIBG (59%), and ^{18}F-FDG (62%).

PGL ruled out

In the four patients in whom PGL was ruled out by biochemical investigation and clinical follow-up, two had

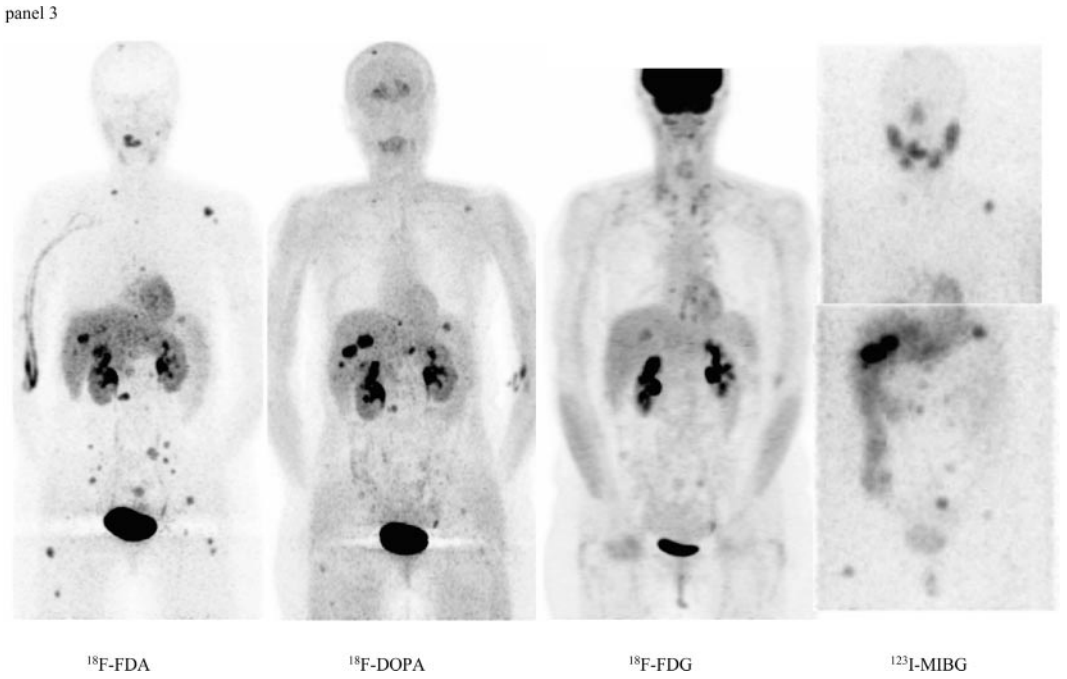

FIG. 1. *Continued.*

false-positive lesions on imaging. One patient (no. n03), a carrier of an *SDHB* mutation (IVS1 + 1G>T), was found to have an 8- × 5-cm gastrointestinal stromal tumor between the stomach and pancreas, which was visualized by CT, MRI, ^{18}F-DOPA PET, and ^{18}F-FDG PET/CT but negative on ^{18}F-FDA PET/CT and ^{123}I-MIBG scintigraphy. In the second patient (no. n01), a 2-cm left adrenal incidentaloma was seen on CT and MRI, which was also visible on ^{18}F-FDG PET/CT.

Discussion

We present the first comprehensive head-to-head comparison between ^{18}F-FDA and ^{18}F-FDG PET/CT, ^{18}F-DOPA PET, and ^{123}I-MIBG scintigraphy for localizing benign and malignant sympathetic PGLs. Nonmetastatic PGLs were equally well localized by these techniques. For the detection of metastases seen on CT, however, ^{18}F-FDA was superior to ^{18}F-DOPA and ^{123}I-MIBG scanning. *SDHB*-related metastatic disease is best detected by ^{18}F-FDG PET/CT, whereas ^{18}F-DOPA PET performs best in non-*SDHB* patients.

Different functional imaging agents target PGL tumor cells through different mechanisms. ^{123}I- and ^{131}I-labeled MIBG and ^{18}F-FDA are actively transported into neurosecretory granules of catecholamine-producing cells via the vesicular monoamine transporters after uptake into cells by the norepinephrine transporter (20). In contrast, ^{18}F-DOPA enters the cell via the amino acid transporter based on the capability of PGL and other neuroendocrine tumors to take up, decarboxylate, and store amino acids and their biogenic amines (20, 21). Instead of targeting catecholamine pathways, ^{18}F-FDG enters the cell via the glucose transporter, and its accumulation is an index of increased glucose metabolism (22, 23).

A biochemical diagnosis of PGL is typically followed by anatomic and functional imaging studies to localize the primary tumor(s) and rule out metastases. ^{123}I/^{131}I-MIBG is the most widely used tracer in the first-line functional imaging of PGL. ^{123}I-MIBG is preferred over ^{131}I-MIBG because of its higher sensitivity, lower radiation exposure, and improved imaging quality with single-photon emission-computed tomography (24). Previous studies suggest a sensitivity of ^{123}I-MIBG scintigraphy of 92–98% for nonmetastatic PGL (15) and 57–79% for metastases (8, 15). The present findings confirm that the sensitivity is high for primary tumors and relatively poor (~50%) for metastases. We feel that the use of ^{123}I-MIBG scintigraphy in patients with metastatic PGL should be limited to the evaluation of whether the patient qualifies for ^{131}I-MIBG treatment.

TABLE 5. *SDHB- vs.* non-*SDHB* metastatic PGL

	SDHB **(15 patients)**	**non-*SDHB*** **(13 patients)**	***P***
^{18}F-DOPA[A]	20% (25/126)	93% (79/85)	<0.001
^{18}F-FDA[B]	82% (103/126)	76% (65/85)	0.037
^{123}I-MIBG[C]	57% (60/106)	59% (48/81)	ns
^{18}F-FDG[D]	83% (105/126)	62% (53/85)	<0.001

Within *SDHB* patients: A *vs.* B, A *vs.* C, A *vs.* D, B *vs.* C, C *vs.* D: $P < 0.01$; B *vs.* D: P = ns. Within non-*SDHB* patients: A *vs.* B, A *vs.* C, A *vs.* D: $P < 0.01$; B *vs.* C: $P = 0.035$; B *vs.* D, C *vs.* D: P = ns.

Apart from its established role the localization of gastrointestinal carcinoid tumors (25–27), ^{18}F-DOPA PET has been suggested to be an excellent alternative for the imaging of sympathetic (10, 28–30) and parasympathetic (11, 31) PGL. In a study of 17 patients, ^{18}F-DOPA PET detected tumors with a strikingly high sensitivity and specificity of both 100% (10). More recent studies confirmed the usefulness of this technique in benign and malignant abdominal PGL (29–32). We also show that ^{18}F-DOPA is a very useful alternative for the specific localization of primary PGL, although it can yield both false-negative and false-positive results. In patients with metastatic disease, a per-lesion-based analysis showed a limited overall sensitivity of ^{18}F-DOPA PET: less than half of the metastases detected by CT/MRI were detected by ^{18}F-DOPA PET. On the other hand, in 71% of patients with malignant PGL, one or more metastases were discerned by the technique. Moreover, a subgroup analysis indicated that its sensitivity is excellent for non-*SDHB* metastases (94%) but poor for *SDHB*-related metastases (20%). This discrepancy remains unexplained. Our results are at variance with a previously published case series, in which ^{18}F-DOPA PET identified more metastases than MIBG single-photon emission-computed tomography and ^{18}F-FDG PET in four of five patients with malignant PGL (31).

^{18}F-FDA was initially developed at the National Institutes of Health for functional imaging of the sympathetic nervous system and later evaluated as a new imaging tool for PGL to optimally discern both primary tumors and metastatic lesions. The present findings confirm the high sensitivity of ^{18}F-FDA PET previously shown for both primary tumors and metastases (13, 33) and show that ^{18}F-FDA PET/CT is superior to ^{18}F-DOPA PET and ^{123}I-MIBG scintigraphy for localizing metastases. In fact, the number of lesions detected by ^{18}F-FDA PET far exceeded the number of lesions on CT and MRI and other functional imaging modalities and were probably underestimated due to truncation of lesion counts, which was necessary in 60% more regions for ^{18}F-FDA PET than for CT and MRI.

We found a surprisingly high sensitivity (88%) of ^{18}F-FDG PET for nonmetastatic PGL. Previously, sensitivities ranging from 58 to 70% have been reported (6, 34). We do not advocate the use of ^{18}F-FDG for the first-line imaging of PGL, because its uptake is not PGL-specific.

The observed differences in radiotracer accumulation between primary tumors and metastases are likely related to differences in tumor cell properties. Theoretically, dedifferentiation might lead to loss of the specific norepinephrine transporters in these tumors, but the avid accumulation of ^{18}F-FDA in the majority of metastatic lesions does not support this theory. Alternatively, tracer accumulation may be directly linked to genotype-specific tumor biology. Malignant potential, tumor location, and biochemical phenotype are all closely linked to underlying mutations in PGL susceptibility genes (35, 36). In previous studies we provided evidence for such a genetic signature on a tumor's tracer dynamics. For instance, we have shown that *VHL* PGLs are better localized with ^{18}F-FDA PET than ^{131}I-MIBG scintigraphy, which may be related to limited expression of norepinephrine transporters by *VHL* PGL cells and a better affinity of ^{18}F-FDA than MIBG for these transporters (17, 37).

Our previous (8) and current observations in patients with *SDHB*-related PGL provide additional evidence for a link between genotype-specific tumor biology and imaging. *SDHB* mutations are associated with PGLs of a particularly high malignant potential (36). In the present study, we confirm that ^{18}F-FDG PET has an excellent sensitivity for *SDHB*-associated metastatic PGL (8, 38). ^{18}F-FDG accumulation is an index of increased tissue glucose metabolism, and, as a marker of tumor viability, the degree of ^{18}F-FDG uptake usually reflects tumor aggressiveness (22). In this study, the high sensitivity of ^{18}F-FDG PET was specific for *SDHB*-related metastases, rather than a feature of PGL metastases in general. Therefore, avid ^{18}F-FDG uptake by PGL does not appear to be merely an indicator of a high metabolic rate due to malignancy *per se* but may rather be directly linked to *SDHB*-specific tumor biology. The *SDHB* gene encodes for subunit B of the mitochondrial succinate dehydrogenase complex II that catalyzes the oxidation of succinate to fumarate in the Krebs cycle and feeds electrons to the respiratory chain ubiquinone pool, which ultimately leads to the generation of ATP (oxidative phosphorylation). *SDHB* mutations can lead to complete loss of succinate dehydrogenase enzymatic activity in malignant PGL, with up-regulation of hypoxic-angiogenetic responsive genes (39). Impairment of mitochondrial function due to loss of *SDHB* function may cause tumor cells to shift from oxidative phosphorylation to aerobic glycolysis, a phenomenon known as the Warburg effect (40). Higher glucose requirement because of a switch to less efficient pathways for cellular energy production may explain the increased ^{18}F-FDG uptake by malignant *SDHB*-related PGL. This possible bioenergenetic signature on imaging awaits confirmation on a molecular level.

Based on our previous findings, we do not recommend the use of ^{111}In-pentetreotide scintigraphy as a first-line imaging tool for PGL (8, 41). Novel somatostatin receptor-based PET scanning using ^{68}Ga-DOTA-peptides (42) awaits further evaluation.

Our findings can assist practicing physicians in choosing the most appropriate type of functional imaging for individual patients with sympathetic, nonhead, and neck

PGL. We recommend the use of ^{18}F-FDA PET/CT in patients with a biochemically established diagnosis of PGL when the aim is to localize the primary tumor(s) and rule out metastases. If ^{18}F-FDA PET/CT is unavailable, ^{18}F-DOPA PET/(CT) or ^{123}I-MIBG scintigraphy can be used. For patients with known metastatic PGL, we recommend the use of ^{18}F-FDA PET in patients with an unknown genotype, ^{18}F-FDG or ^{18}F-FDA PET in *SDHB* mutation carriers, and ^{18}F-DOPA or ^{18}F-FDA PET in non-*SDHB* patients.

Acknowledgments

Address all correspondence and requests for reprints to: Henri J. L. M. Timmers, Department of Endocrinology, Radboud University Nijmegen Medical Center, P.O. Box 9101, 6500 HB Nijmegen, The Netherlands. E-mail: h.timmers@endo.umcn.nl.

This work was supported by the Intramural Research Program of the National Institute of Child Health and Human Development/National Institutes of Health.

Disclosure Summary: The authors have nothing to disclose.

References

1. **DeLellis RA, Lloyd RV, Heitz PU, Eng C** 2004 Pathology and genetics: World Health Organization classification of tumours of endocrine organs. Oxford, UK: Oxford University Press
2. **Lenders JW, Eisenhofer G, Mannelli M, Pacak K** 2005 Phaeochromocytoma. Lancet 366:665–675
3. **Pacak P, Keiser H, Eisenhofer G** 2005 Pheochromocytoma. In: De Groot LJ, Jameson JL, eds. Textbook of endocrinology. Philadelphia: Elsevier Saunders, Inc.; 2501–2534
4. **Lenders JW, Pacak K, Walther MM, Linehan WM, Mannelli M, Friberg P, Keiser HR, Goldstein DS, Eisenhofer G** 2002 Biochemical diagnosis of pheochromocytoma: which test is best? JAMA 287: 1427–1434
5. **Ilias I, Shulkin B, Pacak K** 2005 New functional imaging modalities for chromaffin tumors, neuroblastomas and ganglioneuromas. Trends Endocrinol Metab 16:66–72
6. **Shulkin BL, Thompson NW, Shapiro B, Francis IR, Sisson JC** 1999 Pheochromocytomas: imaging with 2-[fluorine-18]fluoro-2-deoxy-D-glucose PET. Radiology 212:35–41
7. **Taniguchi K, Ishizu K, Torizuka T, Hasegawa S, Okawada T, Ozawa T, Iino K, Taniguchi M, Ikematsu Y, Nishiwaki Y, Kida H, Waki S, Uchimura M** 2001 Metastases of predominantly dopamine-secreting phaeochromocytoma that did not accumulate metaiodobenzylguanidine: imaging with whole body positron emission tomography using 18F-labelled deoxyglucose. Eur J Surg 167:866–870
8. **Timmers HJ, Kozupa A, Chen CC, Carrasquillo JA, Ling A, Eisenhofer G, Adams KT, Solis D, Lenders JW, Pacak K** 2007 Superiority of fluorodeoxyglucose positron emission tomography to other functional imaging techniques in the evaluation of metastatic SDHB-associated pheochromocytoma and paraganglioma. J Clin Oncol 25:2262–2269
9. **Bhatia KS, Ismail MM, Sahdev A , Rockall AG, Hogarth K, Canizales A, Avril N, Monson JP, Grossman AB, Reznek RH** 2008 (123)I-metaiodobenzylguanidine (MIBG) scintigraphy for the detection of adrenal and extra-adrenal phaeochromocytomas: CT and MRI correlation. Clin Endocrinol (Oxf) 69:181–188
10. **Hoegerle S, Nitzsche E, Altehoefer C, Ghanem N, Manz T, Brink I, Reincke M, Moser E, Neumann HP** 2002 Pheochromocytomas: detection with 18F DOPA whole body PET—initial results. Radiology 222:507–512
11. **Hoegerle S, Ghanem N, Altehoefer C, Schipper J, Brink I, Moser E, Neumann HP** 2003 18F-DOPA positron emission tomography for the detection of glomus tumours. Eur J Nucl Med Mol Imaging 30:689–694
12. **Pacak K, Goldstein DS, Doppman JL, Shulkin BL, Udelsman R, Eisenhofer G** 2001 A "pheo" lurks: novel approaches for locating occult pheochromocytoma. J Clin Endocrinol Metab 86:3641–3646
13. **Pacak K, Eisenhofer G, Carrasquillo JA, Chen CC, Li ST, Goldstein DS** 2001 6-[18F]fluorodopamine positron emission tomographic (PET) scanning for diagnostic localization of pheochromocytoma. Hypertension 38:6–8
14. **van der Harst E, de Herder WW, Bruining HA, Bonjer HJ, de Krijger RR, Lamberts SW, van de Meiracker AH, Boomsma F, Stijnen T, Krenning EP, Bosman FT, Kwekkeboom DJ** 2001 [(123)I]-metaiodobenzylguanidine and [(111)In]-octreotide uptake in benign and malignant pheochromocytomas. J Clin Endocrinol Metab 86:685–693
15. **Van Der Horst-Schrivers AN, Jager PL, Boezen HM, Schouten JP, Kema IP, Links TP** 2006 Iodine-123 metaiodobenzylguanidine scintigraphy in localising phaeochromocytomas—experience and meta-analysis. Anticancer Res 26:1599–1604
16. **Amar L, Bertherat J, Baudin E, Ajzenberg C, Bressac-de Paillerets B, Chabre O, Chamontin B, Delemer B, Giraud S, Murat A, Niccoli-Sire P, Richard S, Rohmer V, Sadoul JL, Strompf L, Schlumberger M, Bertagna X, Plouin PF, Jeunemaitre X, Gimenez-Roqueplo AP** 2005 Genetic testing in pheochromocytoma or functional paraganglioma. J Clin Oncol 23:8812–8818
17. **Kaji P, Carrasquillo JA, Linehan WM, Chen CC, Eisenhofer G, Pinto PA, Lai EW, Pacak K). et al** 2007 The role of 6-[18F]fluorodopamine positron emission tomography in the localization of adrenal pheochromocytoma associated with von Hippel-Lindau syndrome. Eur J Endocrinol 156:483–487
18. **Linnoila RI, Keiser HR, Steinberg SM, Lack EE** 1990 Histopathology of benign versus malignant sympathoadrenal paragangliomas: clinicopathologic study of 120 cases including unusual histologic features. Hum Pathol 21:1168–1180
19. **Timmers HJ, Hadi M, Carrasquillo JA, Chen CC, Martiniova L, Whatley M, Ling A, Eisenhofer G, Adams KT, Pacak K** 2007 The effects of carbidopa on uptake of 6–18F-fluoro-L-DOPA in PET of pheochromocytoma and extraadrenal abdominal paraganglioma. J Nucl Med 48:1599–1606
20. **Eisenhofer G** 2001 The role of neuronal and extraneuronal plasma membrane transporters in the inactivation of peripheral catecholamines. Pharmacol Ther 91:35–62
21. **Pearse AG** 1969 The cytochemistry and ultrastructure of polypeptide hormone-producing cells of the APUD series and the embryologic, physiologic and pathologic implications of the concept. J Histochem Cytochem 17:303–313
22. **Belhocine T, Spaepen K, Dusart M, Castaigne C, Muylle K, Bourgeois P, Bourgeois D, Dierickx L, Flamen P** 2006 18FDG PET in oncology: the best and the worst. Int J Oncol 28:1249–1261 (Review)
23. **Pauwels EK, Sturm EJ, Bombardieri E, Cleton FJ, Stokkel MP** 2000 Positron-emission tomography with [18F]fluorodeoxyglucose. Part I. Biochemical uptake mechanism and its implication for clinical studies. J Cancer Res Clin Oncol 126:549–559
24. **Lynn MD, Shapiro B, Sisson JC, Beierwaltes WH, Meyers LJ, Ackerman R, Mangner TJ** 1985 Pheochromocytoma and the normal adrenal medulla: improved visualization with I-123 MIBG scintigraphy. Radiology 155:789–792
25. **Becherer A, Szabo M, Karanikas G, Wunderbaldinger P, Angelberger P, Raderer M, Kurtaran A, Dudczak R, Kletter K**

2004 Imaging of advanced neuroendocrine tumors with (18)F-FDOPA PET. J Nucl Med 45:1161–1167
26. **Hoegerle S, Altehoefer C, Ghanem N, Koehler G, Waller CF, Scheruebl H, Moser E, Nitzsche E** 2001 Whole-body 18F dopa PET for detection of gastrointestinal carcinoid tumors. Radiology 220: 373–380
27. **Nanni C, Rubello D, Fanti S** 2006 18F-DOPA PET/CT and neuroendocrine tumours. Eur J Nucl Med Mol Imaging 33:509–513
28. **Brink I, Schaefer O, Walz M, Neumann HP** 2006 Fluorine-18 DOPA PET imaging of paraganglioma syndrome. Clin Nucl Med 31:39–41
29. **Imani F, Agopian VG, Auerbach MS, Walter MA, Imani F, Benz MR, Dumont RA, Lai CK, Czernin JG, Yeh MW** 2009 18F-FDOPA PET and PET/CT accurately localize pheochromocytomas. J Nucl Med 50:513–519
30. **Fiebrich HB, Brouwers AH, Kerstens MN, Pijl ME, Kema IP, de Jong JR, Jager PL, Elsinga PH, Dierckx RA, van der Wal JE, Sluiter WJ, de Vries EG, Links TP** 2009 18F-DOPA PET is superior to conventional imaging with 123I-metaiodobenzylguanidine scintigraphy, CT, and MRI in localizing tumors causing catecholamine excess. J Clin Endocrinol Metab 94:3922–3930
31. **Taieb D, Tessonnier L, Sebag F , Niccoli-Sire P, Morange I, Colavolpe C, De Micco C, Barlier A, Palazzo FF, Henry JF, Mundler O** 2008 The role of 18F-FDOPA and 18F-FDG-PET in the management of malignant and multifocal phaeochromocytomas. Clin Endocrinol (Oxf) 69:580–586
32. **Mackenzie IS, Gurnell M, Balan KK, Simpson H, Chatterjee K, Brown MJ** 2007 The use of 18-fluoro-dihydroxyphenylalanine and 18-fluorodeoxyglucose positron emission tomography scanning in the assessment of metaiodobenzylguanidine-negative phaeochromocytoma. Eur J Endocrinol 157:533–537
33. **Ilias I, Yu J, Carrasquillo JA, Chen CC, Eisenhofer G, Whatley M, McElroy B, Pacak K** 2003 Superiority of 6-[18F]fluorodopamine positron emission tomography versus [131I]metaiodobenzylguanidine scintigraphy in the localization of metastatic pheochromocytoma. J Clin Endocrinol Metab 88:4083–4087
34. **Mann GN, Link JM, Pham P, Pickett CA, Byrd DR, Kinahan PE, Krohn KA, Mankoff DA** 2006 [11C]metahydroxyephedrine and [18F]fluorodeoxyglucose positron emission tomography improve clinical decision making in suspected pheochromocytoma. Ann Surg Oncol 13:187–197
35. **Eisenhofer G, Walther MM, Huynh TT, Li ST, Bornstein SR, Vortmeyer A, Mannelli M, Goldstein DS, Linehan WM, Lenders JW, Pacak K** 2001 Pheochromocytomas in von Hippel-Lindau syndrome and multiple endocrine neoplasia type 2 display distinct biochemical and clinical phenotypes. J Clin Endocrinol Metab 86:1999–2008
36. **Timmers HJ, Kozupa A, Eisenhofer G, Raygada M, Adams KT, Solis D, Lenders JW, Pacak K** 2007 Clinical presentations, biochemical phenotypes, and genotype-phenotype correlations in patients with succinate dehydrogenase subunit B-associated pheochromocytomas and paragangliomas. J Clin Endocrinol Metab 92:779–786
37. **Huynh TT, Pacak K, Brouwers FM, Abu-Asab MS, Worrell RA, Walther MM, Elkahloun AG, Goldstein DS, Cleary S, Eisenhofer G** 2005 Different expression of catecholamine transporters in phaeochromocytomas from patients with von Hippel-Lindau syndrome and multiple endocrine neoplasia type 2. Eur J Endocrinol 153:551–563
38. **Taieb D, Sebag F, Barlier A, Tessonnier L, Palazzo FF, Morange I, Niccoli-Sire P, Fakhry N, De Micco C, Cammilleri S, Enjalbert A, Henry JF, Mundler O** 2009 18F-FDG avidity of pheochromocytomas and paragangliomas: a new molecular imaging signature? J Nucl Med 50:711–717
39. **Gimenez-Roqueplo AP, Favier J, Rustin P, Rieubland C, Kerlan V, Plouin PF, Rötig A, Jeunemaitre X** 2002 Functional consequences of a SDHB gene mutation in an apparently sporadic pheochromocytoma. J Clin Endocrinol Metab 87:4771–4774
40. **Warburg O** 1956 On the origin of cancer cells. Science 123:309–314
41. **Ilias I, Chen CC, Carrasquillo JA, Whatley M, Ling A, Lazúrová I, Adams KT, Perera S, Pacak K** 2008 Comparison of 6–18F-fluorodopamine PET with 123I-metaiodobenzylguanidine and 111in-pentetreotide scintigraphy in localization of nonmetastatic and metastatic pheochromocytoma. J Nucl Med 49:1613–1619
42. **Fanti S, Ambrosini V, Tomassetti P, Castellucci P, Montini G, Allegri V, Grassetto G, Rubello D, Nanni C, Franchi R** 2008 Evaluation of unusual neuroendocrine tumours by means of 68Ga-DOTA-NOC PET. Biomed Pharmacother 62:667–671